Identification of a basement membrane-related gene signature for predicting prognosis, immune infiltration, and drug sensitivity in colorectal cancer

Xiang Shengxiao[1†], Sun Xinxin[2†], Zhu Yunxiang[3],
Tang Zhijie[3] and Tang Xiaofei[3*]

[1]Department of Science and Education, Suqian First Hospital, Suqian, Jiangsu, China, [2]Department of
Science and Education, Yangzhou Maternal and Child Health Hospital, Yangzhou, Jiangsu, China,
[3]Department of Gastrointestinal Surgery, The Affiliated Hospital of Yangzhou University, Yangzhou
University, Yangzhou, China

Background: Colorectal cancer (CRC) is the most common malignancy affecting the gastrointestinal tract. Extensive research indicates that basement membranes (BMs) may play a crucial role in the initiation and progression of the disease.

Methods: Data on the RNA expression patterns and clinicopathological information of patients with CRC were sourced from The Cancer Genome Atlas (TCGA) and the Gene Expression Omnibus (GEO) databases. A BM-linked risk signature for the prediction of overall survival (OS) was formulated using univariate Cox regression and combined machine learning techniques. Survival outcomes, functional pathways, the tumor microenvironment (TME), and responses to both immunotherapy and chemotherapy within varying risk classifications were also investigated. The expression trends of the model genes were evaluated by reverse transcription polymerase chain reaction (RT-PCR) and the Human Protein Atlas (HPA) database.

Results: A nine-gene risk signature containing UNC5C, TINAG, TIMP1, SPOCK3, MMP1, AGRN, UNC5A, ADAMTS4, and ITGA7 was constructed for the prediction of outcomes in patients with CRC. The expression profiles of these candidate genes were verified using RT-PCR and the HPA database and were found to be consistent with the findings on differential gene expression in the TCGA dataset. The validity of the signature was confirmed using the GEO cohort. The patients were stratified

into different risk groups according to differences in clinicopathological characteristics, TME features, enrichment functions, and drug sensitivities. Lastly, the prognostic nomogram model based on the risk score was found to be effective in identifying high-risk patients and predicting OS.

Conclusion: A basement membrane-related risk signature was constructed and found to be effective for predicting the prognosis of patients with CRC.

Introduction

Colorectal cancer (CRC) is a prevalent malignancy affecting the gastrointestinal tract. In 2023, approximately 153 000 individuals in the USA were diagnosed with CRC, with nearly 52 000 succumbing to the disease (1). Over time, a spectrum of therapeutic modalities for CRC, encompassing surgery, radiation, and chemotherapy, have significantly improved patient prognoses (2). Nonetheless, these interventions do not always yield favorable results. Certain individuals experience suboptimal outcomes attributable to cancer recurrence, metastasis, or drug resistance (3–5). Molecular alterations, both genetic and non-genetic, contribute substantially to both the onset and progression of CRC. Hence, it is imperative to pinpoint novel biomarkers for improving treatment efficacy and develop predictive models to steer the management of patients with CRC.

The basement membrane (BM) represents a distinctive form of extracellular matrix (ECM) that surrounds cells. The BM is composed predominantly of collagen IV, laminin, proteoglycans, nidogens, and growth factors (6, 7). A fully intact BM is essential for preventing the infiltration of tumor cells into the surrounding stromal tissue, and thus acts as a critical physical barrier to tumor cell metastasis (7, 8). Dysregulation of the BM can increase tumor cell migration and invasiveness (9). Moreover, several studies have reported that the BM can control the differentiation, cell polarity, and survival of tumor cells (10, 11). A study by Jayadev and his team observed a network of 222 BM-related genes (BMGs), highlighting the complex nature of the BM and how it can affect human health (12). Certain features of the BM have been demonstrated to impact the prognosis of patients with liver, stomach, and breast cancer (13–15). Despite this, no studies have investigated whether these BMGs could affect the survival rates of patients with CRC.

In this study, we constructed a predictive model that incorporated nine BMGs to estimate survival outcomes for patients with CRC. This model also sheds light on the status of the tumor microenvironment (TME) and predicts how the patient might respond to chemotherapy.

The findings provide novel insights for prognostic evaluation and decision-making in the management of patients with CRC. Moreover, they open new avenues for exploring more effective treatment strategies for patients with CRC.

# Materials and methods

Study design

Figure 1 illustrates a flowchart of the study, providing a comprehensive overview of the entire study process.

Data collection and preparation

Data on the RNA expression patterns and clinicopathological information of 624 CRC tissues and 51 normal colonic tissues were acquired from The Cancer Genome Atlas (TCGA) database. Additional data were obtained from the GSE29621 dataset from the Gene Expression Omnibus (GEO) database; these data were used as the validation set (16, 17). The TCGA-CRC dataset was incorporated with the GEO data and the "ComBat" algorithm from the "sva" R package was used for the correction of batch effects.

Identification of differentially expressed genes

A set of 224 BMGs was obtained from a previous study for subsequent analysis (12). Differentially expressed BMGs (DEBMGs) between normal and tumor samples were identified using the R package "limma". Using the criteria of an absolute log2 fold-change (FC) above 1 and a false discovery rate (FDR) below 0.05, a total of 89 DEBMGs were identified.

FIGURE 1
Study Flow Diagram.
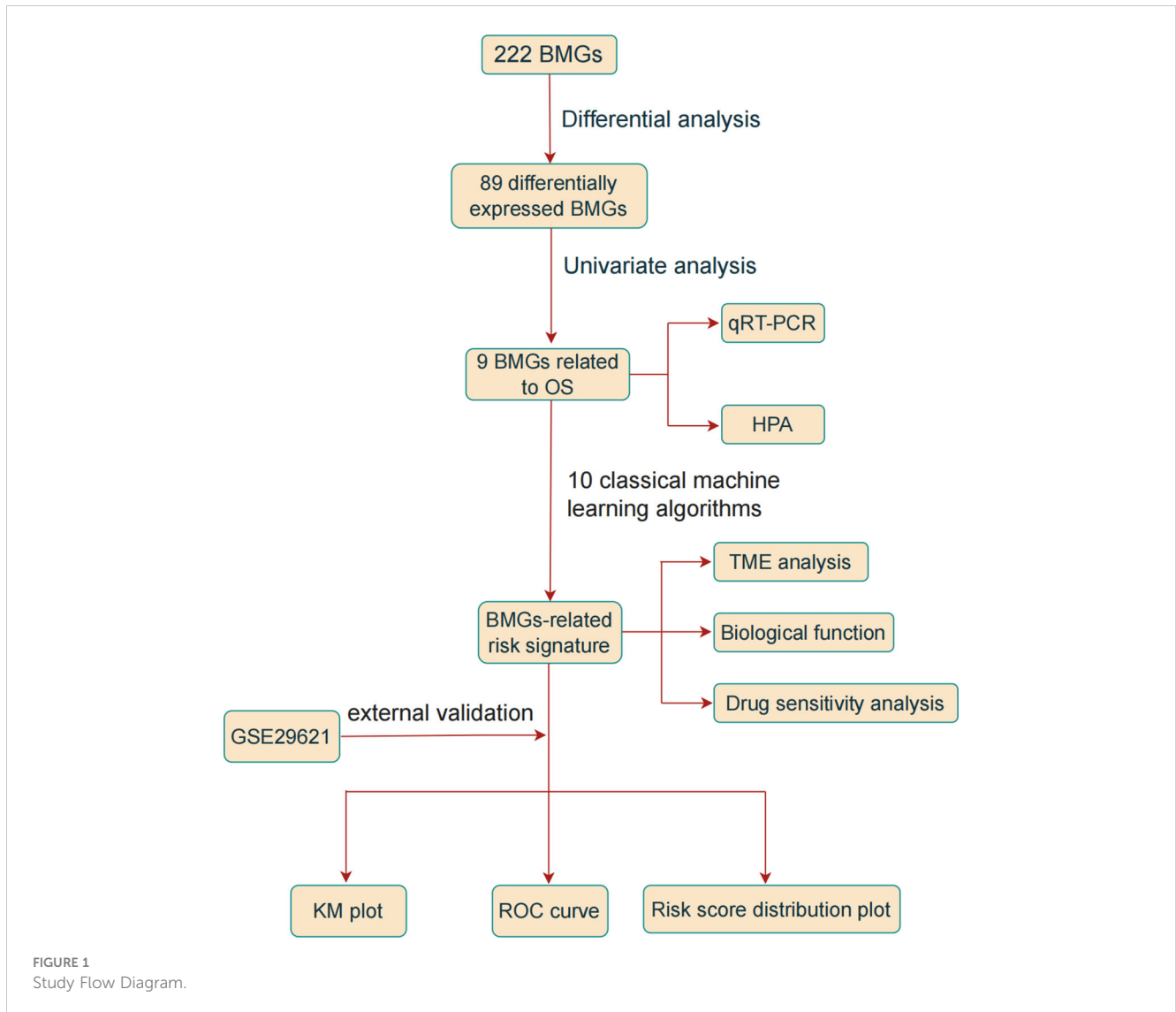
Establishment of a prognostic model for BM

To investigate the associations between the identified DEBMGs and the overall survival (OS) rates of patients with CRC, a univariate Cox regression analysis was conducted to identify prognostic markers, using the criterion of a p-value less than 0.05, signifying statistical significance.

A comprehensive analytical process was then followed, integrating 10 classical machine-learning algorithms and 117 algorithm combinations to devise an accurate and robust prognostic signature derived from characteristics of the BM (18). These algorithms included supervised principal components (SuperPC), random forest (RF), CoxBoost, least absolute shrinkage and selection operator (LASSO), survival support vector machine (Survival-SVM), partial least squares regression for Cox (plsRcox), gradient boosting machine (GBM), ridge regression, elastic network (Enet), and Stepwise Cox. The efficacy of each model was assessed using the concordance index (C-index) for both the training and validation sets, and the model with the top average C-index was considered the most suitable.

Analysis of the tumor microenvironment and gene set variation analysis

The "ESTIMATE" package in R was used to analyze the TME in terms of different risk categories (19). In parallel, immune cell infiltration was assessed using single-sample gene set enrichment analysis (ssGSEA) from the "gsva" package in R. Furthermore, 50 hallmark gene sets were identified from the MsigDB database and the gene set variation analysis (GSVA) algorithm was used for the comprehensive evaluation of each gene set, thereby assessing potential changes in the biological functions of the different risk groups (20).

Therapy response prediction

The TIDE computational method was employed to analyze the likelihood of patients with CRC responding to immunotherapy. A higher TIDE score indicates an increased chance of evading immune response during such therapy (21). Furthermore, the "Oncopredict" package was used to predict the response of patients with CRC to commonly prescribed medications (22).

Exploration of expression patterns

Human intestinal epithelial cells (FHCs) and the human colorectal cancer cell line HCT8 were procured from Punosai Life Science and Technology Co., Ltd. The cells were cultured in DMEM, supplemented with 10% fetal bovine serum, and maintained at 37°C under a 5% CO_2 environment. RNA isolation was performed using TRIzol reagent, followed by reverse transcription with PrimeScript™ RT Master Mix. The housekeeping gene, GAPDH, was used as an internal control. The sequences of the primers are presented in Table 1. Immunohistochemical information from the HPA database was used to investigate the protein expression of the genes.

TABLE 1 Primers used for RT-PCR.

Gene symbol	Primer sequence (5′ to 3′)
ITGA7	Forward: TGCTGGTGCTGCTCCTGTG
	Reverse: TCTTCTCCTCCTTGAACTGCTGTC
ADAMTS4	Forward: CTGACTTCCTGGACAATGGCTATG
	Reverse: GCTGTGGACAATGGCGTGAG
UNC5A	Forward: GCCGTCTGCCTGGTCCTG
	Reverse: TGGAAGCCTGAGGTGAGAATGG
AGRN	Forward: GATGGAGTCACATACGGCAACG
	Reverse: TCACAGTCACGGAGGCAGATG
MMP1	Forward: TTACACGCCAGATTTGCCAAGAG
	Reverse: TTACACGCCAGATTTGCCAAGAG
SPOCK3	Forward: AATAATGAGTGGTGCTACTGCTTCC
	Reverse: TGCCGCTTCTGAATATTGCTGAG
TIMP1	Forward: CCTGTTGTTGCTGTGGCTGATAG
	Reverse: ACGCTGGTATAAGGTGGTCTGG
UNC5C	Forward: CGGACTGGGACTGGGATACTTG
	Reverse: GAGGCTCAGGTGGATCAGAAGG
TINAG	Forward: TATGCGGCGAATGCGTTGTG
	Reverse: TACCAAGGCTGTGTGTGAGGAG
GAPDH	Forward: GGAGCGAGATCCCTCCAAAAT
	Reverse: GGCTGTTGTCATACTTCTCATGG

Statistical analysis

R software (version 4.1.1) was used for all data analysis and for generating visual illustrations. Two-sided P-values <0.05 were considered statistically significant.

Results

Identification of DEBMGs and development of the prognostic signature

In the initial assessment, the expression patterns of 224 BMGs in both tumor and normal samples were examined in the TCGA-CRC cohort. Analysis of differential expression led to the identification of 89 DEBMGs, 46 of which were upregulated and 42 downregulated (Figure 2A). Subsequently, nine DEBMGs that were shown by univariate Cox regression to be significantly associated with OS were identified (Figure 2B). After the implementation of 117 algorithm combinations for the development of the prediction model, the mean C-index was calculated for each algorithm in the TCGA-CRC and GSE29621 datasets. As depicted in Figures 2C, D, RF was selected as the best model due to its superior average C-index of 0.782.

Evaluation of the performance of the BMG-related risk signature

To assess the prognostic performance of the BMG-related model, patients were stratified into high- and low-risk categories using the median risk score as the cutoff. The Kaplan-Meier (KM) curve demonstrated that the high-risk group displayed markedly worse survival outcomes (Figure 3A). The areas under the receiver operating characteristic (ROC) curve (AUCs) for 1-, 3-, and 5-year OS were 0.981, 0.977, and 0.975, respectively (Figure 3B). In addition, the visual representation of risk score distribution clearly showed that patients classified as high-risk had significantly higher mortality rates (Figure 3C). These findings were confirmed in the validation set, underscoring the consistent and robust performance of the BMG-related risk signature (Figure 3D–F).

Investigation of the association between the risk profile and clinical data indicated significant differences in the TNM stage, venous infiltration, and lymphatic penetration between the high- and low-risk groups. These findings suggest that the risk profile related to BMGs could potentially serve as a predictive marker for clinical traits in patients with CRC (Figures 4A–F).

The TME and functional analysis

The ESTIMATE algorithm was used to examine the relationship between the TME and the BMG-related risk signature. Notably, patients in the high-risk group showed
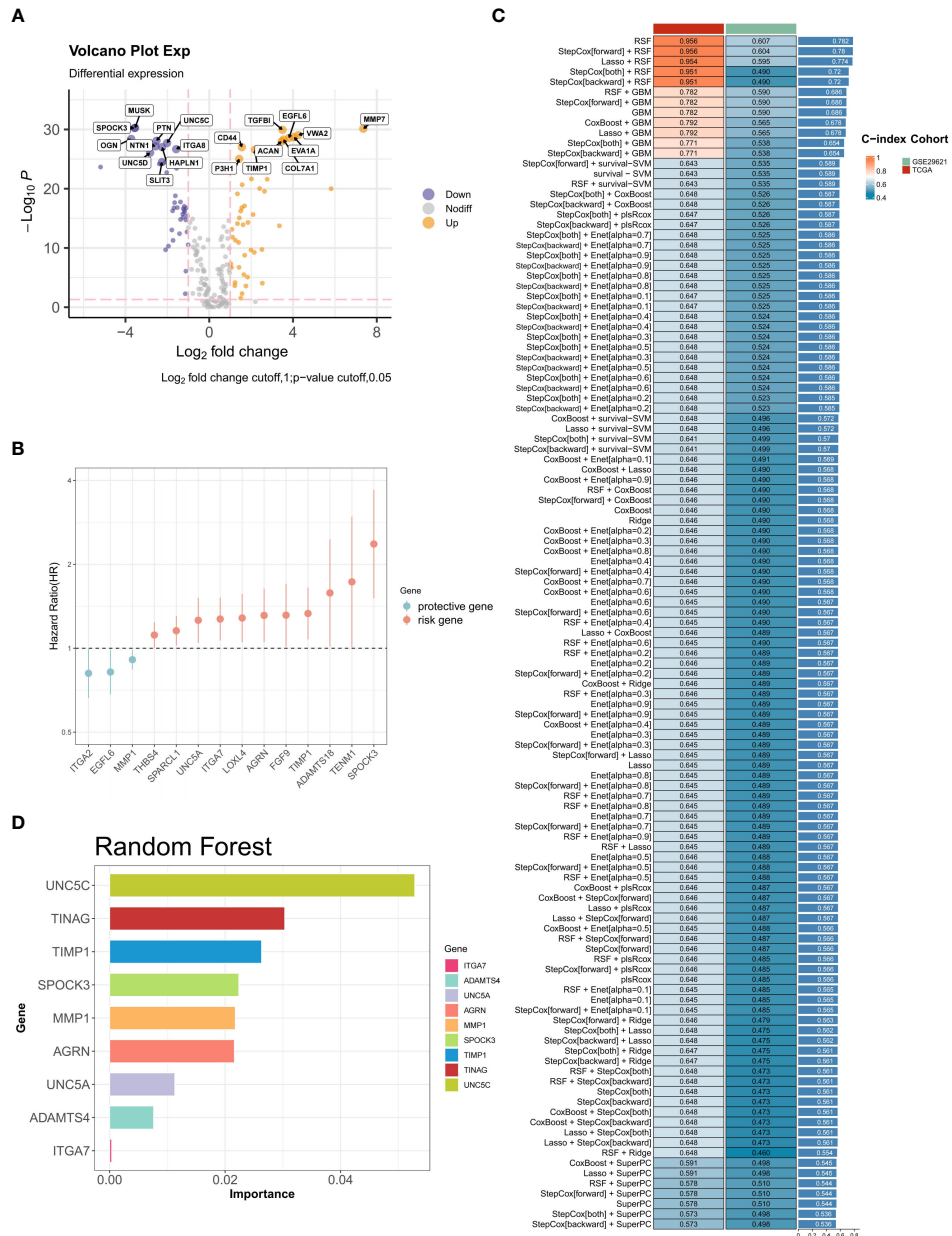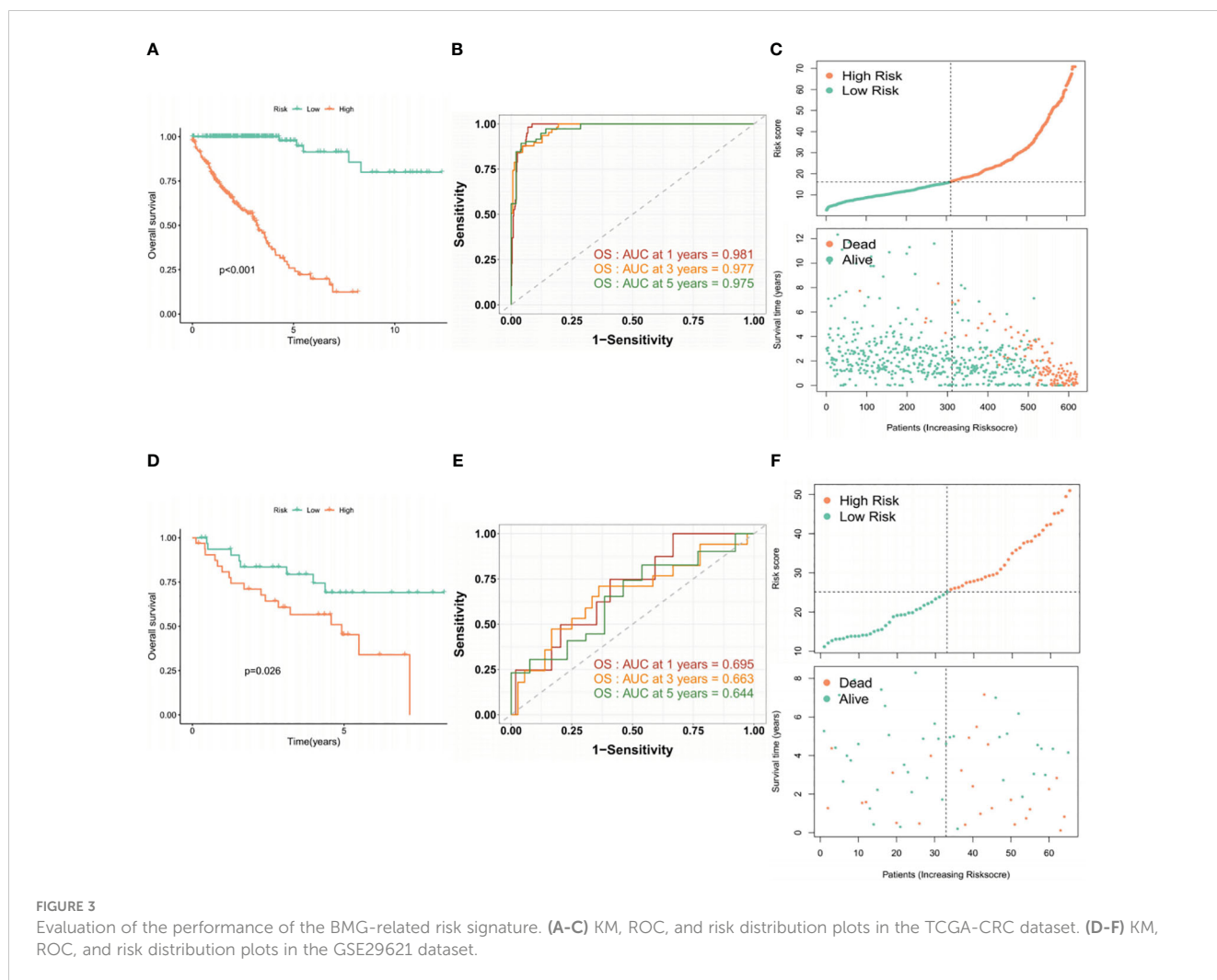
FIGURE 2

Construction of BM-related risk features. **(A)** Volcano plot of the levels of differentially expressed BMGs. **(B)** Univariate Cox regression analysis. **(C, D)** RF was chosen as the best model with the highest average C-index.

significantly elevated stromal and immune scores, along with decreased tumor purity, in contrast to patients categorized as low-risk (Figures 5A–C). This implies that patients with an increased BMG-related risk score had a more active and resilient immune response. Furthermore, the ssGSEA algorithm provided additional evidence by confirming substantial disparities in the immune cell infiltration levels between the two patient cohorts (Figure 5D). Specifically, the high-risk TCGA-CRC group showed significant increases in the infiltration of macrophages, mast cells, and type 1 T helper cells, together with marked reductions in the proportions of CD4+ T cells, activated dendritic cells, and CD56 bright natural killer cells. Lastly, the GSVA method to investigate alterations in hallmark pathway enrichments between the two risk

groups (Figure 5E). Notably, 33 tumor-associated hallmark pathways (66%) exhibited significant enrichment in the high-risk groups, indicating a higher likelihood of tumor cell invasion in these patients.

Drug sensitivity analysis

The TIDE algorithm was used to assess the ability of the BMG-related risk score to predict patient response to cancer immunotherapy. This showed significantly elevated TIDE scores in the high-risk group, indicating a potentially higher likelihood of positive responses to immunotherapy (Figure 6A). To confirm the

FIGURE 3
Evaluation of the performance of the BMG-related risk signature. **(A-C)** KM, ROC, and risk distribution plots in the TCGA-CRC dataset. **(D-F)** KM, ROC, and risk distribution plots in the GSE29621 dataset.

association between the BMG-related risk signature and its clinical application, the "oncoPredict" tool was used to assess the sensitivities to commonly used chemotherapy drugs. A decreased IC50 value implies heightened drug sensitivity and a more favorable therapeutic outcome. The findings indicated that the low-risk group was predicted to be more sensitive to ocittinib, lapatinib, and cyclophosphamide, while the high-risk group showed greater sensitivity to mitoxantrone and epirubicin (Figures 6B–F).

RT-PCR and HPA

The expression of 9 BMGs was verified in the FHC human intestinal epithelial cell and HCT8 human colorectal cancer cell lines using RT-PCR. Increased expression of TIMP1, MMP1, AGRN, UNC5A, and ADAMTS4 was observed, while the expression of UNC5C, TINAG, SPOCK3, and ITGA7 was reduced in the normal FHC cells compared to the HCT8 tumor cells (Figure 7).

Additionally, protein expression of the BMGs was explored using the HPA tool. The protein expression of ADAMTS4, AGRN,

ITGA7, TIMP1, and TINAG was consistent with the PCR results. Unfortunately, the HPA database did not provide any data on the expression of MMP1, SPOCK3, UNC5A, and UNC5C (Figure 8).

Nomogram construction and evaluation

Both univariate and multivariable Cox regression analyses were performed to identify independent predictors of prognosis for patients with CRC. The results of the univariate Cox analysis indicated that age, TNM stage, lymphatic invasion, venous invasion, and the BMG-related risk signature were significantly associated with CRC prognosis (Figure 9A). Subsequently, the multivariable Cox regression analysis identified age, stages N and M, and the risk signature as independent prognostic factors for CRC patients (Figure 9B). These findings were used to construct a nomogram to predict the likelihood of OS for CRC patients at the 1-, 3-, and 5-year time points (Figure 9C). The calibration curve showed a high level of agreement between the predicted survival rates from the nomogram and actual survival rates (Figure 9D).
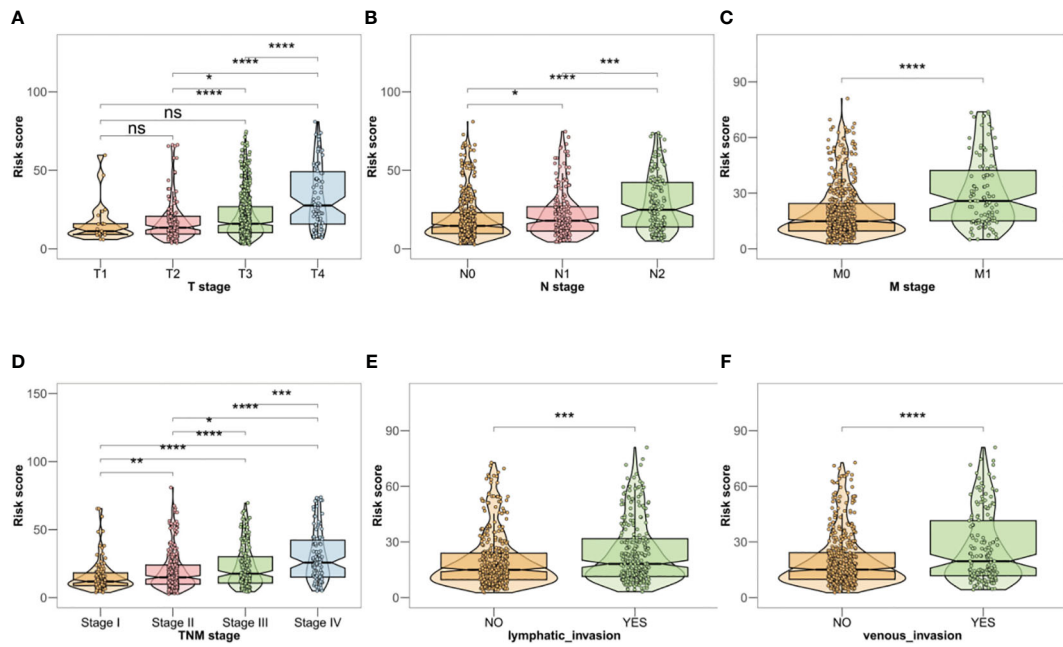
FIGURE 4
(A–F) Clinical correlation analysis in TCGA-CRC database. *P < 0.05, **P < 0.01, ***P < 0.001, ****P < 0.0001, ns, no significant.
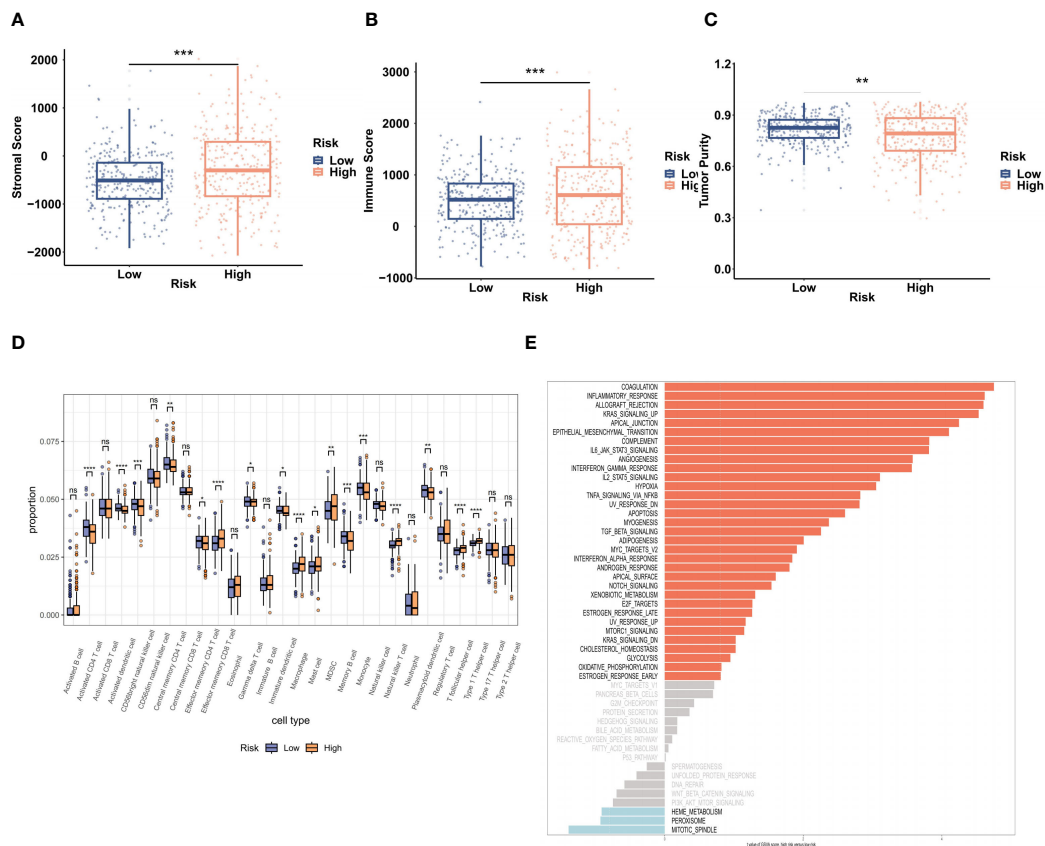

FIGURE 5
Evaluation of the TME and biological functions. (A–C) The stromal score, immune score, and tumor purity in the two risk groups were evaluated by ESTIMATE analysis. (D) ssGSEA analysis of the infiltration of 28 immune cell types. (E) GSVA of 50 hallmark pathway enrichments. **P < 0.01, ***P < 0.001.
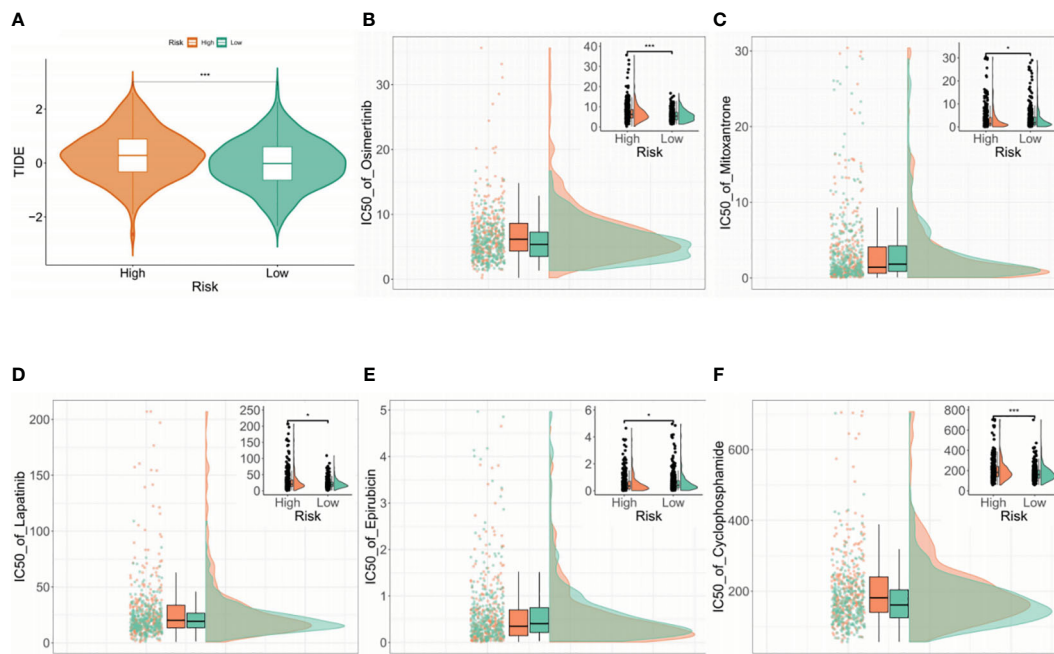
FIGURE 6
Drug sensitivity analysis **(A)** Comparison of TIDE scores between the high- and low-risk groups. **(B–F)** Drug sensitivity analysis of the two groups using the "oncoPredict" tool.
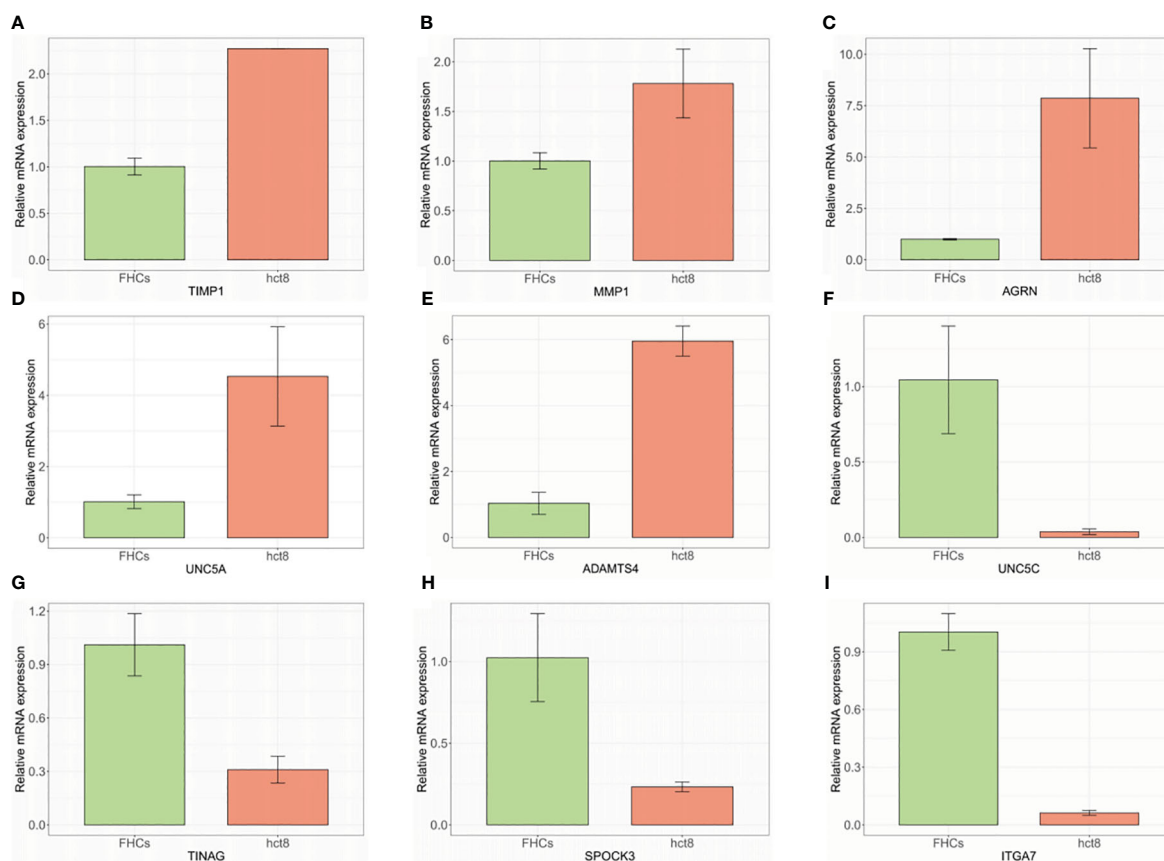

FIGURE 7
(A–I) mRNA levels of BMGs in HCT8 CRC and normal FHC cells measured by RT-PCR.
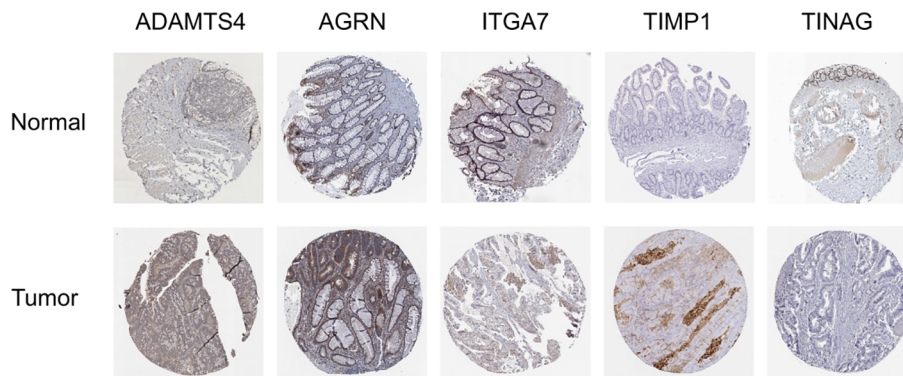
FIGURE 8
Immunohistochemical results from the HPA database.

Discussion

CRC is the most common malignancy of the gastrointestinal tract. The occurrence of distant metastasis is a critical determinant of the disease prognosis (23). Extensive evidence has confirmed that tumor metastasis is frequently associated with the degradation or disruption of the BM (7, 8). Moreover, the BM is involved in the regulation of various cell functions, such as cell polarity, differentiation, and survival (10, 11). The development of risk scores with specific attributes to evaluate the prognosis of CRC patients from various angles has been demonstrated as a feasible approach (24). However, to date, there is a lack of CRC prognostic
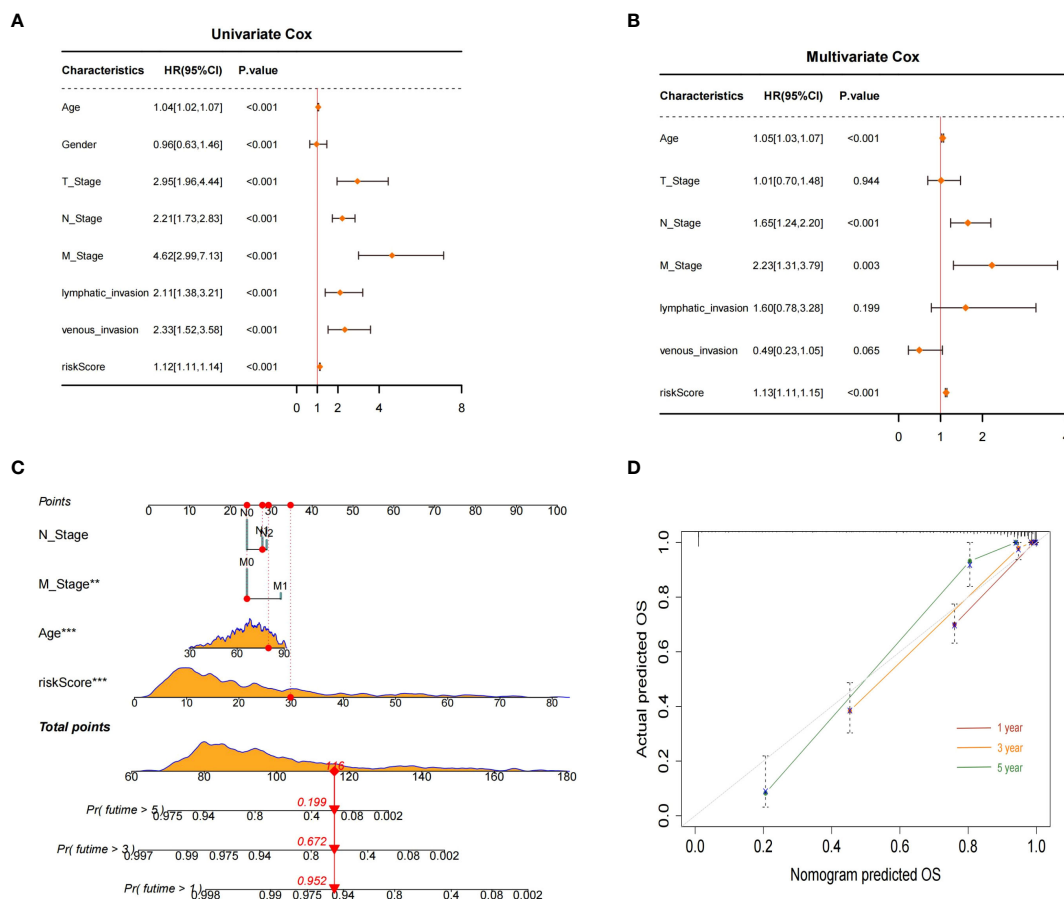

FIGURE 9
Nomogram construction and evaluation. **(A, B)** Univariate and multivariate Cox analyses. **(C)** Nomogram for predicting 1-, 3-, and 5-year OS probabilities for patients with CRC. **(D)** Calibration plot of the nomogram.

models that incorporate the BM. The present study identified nine differentially expressed BMGs that were linked to CRC prognosis. Integration of 10 machine learning algorithms led to the development of a novel prognostic model based on the BMGs, which was found to be effective for predicting the prognosis of patients with CRC. Furthermore, the risk signature could accurately predict both clinicopathological features associated with prognosis and the sensitivity of patients to drugs commonly used for treating CRC.

Previous research has shown that all these BMGs play crucial roles in tumorigenesis and tumor progression. TINAG, an extracellular matrix protein expressed in the BM, has recently been found by Zhang et al. to be involved in the migration, proliferation, and invasion of hepatocellular carcinoma (25). UNC5C, identified as downregulated in CRC, acts as a tumor suppressor and is linked to tumor progression in colorectal malignancies (26, 27). MMP1 is known to be overexpressed in various cancer types and associated with both tumor development and metastasis and, intriguingly, surfaced as a defensive element against CRC (28–30). ADAMTS4, a member of the ADAMTS family, has been shown to promote tumorigenesis in glioblastomas, melanoma, prostate cancer, and other cancers (31–33), while ITGA7, another ECM-binding protein, was found by Liu et al. to inhibit CRC cell growth and metastasis (34) and UNC5A serves as a transmembrane receptor, mediating ligand-dependent signaling pathways that regulate cell survival or induce cell death (35).

Originally recognized as a facilitator of N-type acetylcholine receptors at the neuromuscular junction, AGRN is expressed in the cell membrane where it is involved in controlling neuromuscular communication (36). Zhang et al. discovered that AGRN promotes the progression of lung cancer through the Notch signaling pathway activation, suggesting its potential as a therapeutic target (37). TIMP1 has been found to regulate various tumorigenic processes, including proliferation, apoptosis, and metastasis (38). In Song's research, a strong association between TIMP1 overexpression and CRC recurrence and aggressiveness was demonstrated, highlighting its potential as a viable biomarker for prognosis prediction in CRC (39). SPOCK3, a proteoglycan, is secreted into the extracellular matrix, and Luo et al. reported that SPOCK3 was associated with prostate cancer progression by controlling the infiltration of immune cells (40).

Our research has several limitations that should be acknowledged. Firstly, the study population comprised CRC samples obtained from publicly available databases. Hence, it is important to verify the precision of the BMG risk signature in practical CRC cohorts. Furthermore, despite verification of the expression of BMGs through PCR and immunohistochemistry, the precise mechanisms underlying the functions of these genes in CRC are still not fully understood, requiring additional clarification through *in vivo* and *in vitro* studies.

In summary, a novel BM-related scoring system was constructed that could effectively predict the prognosis of patients with CRC. This scoring system has potential as a valuable tool for guiding clinical treatment decisions, providing clinicians with a reliable reference for personalized treatment strategies. These findings have the potential to significantly advance the development of tailored therapeutic approaches for CRC.

Data availability statement

The original contributions presented in the study are included in the article/supplementary material. Further inquiries can be directed to the corresponding author.

Ethics statement

Ethical approval was not required for the studies on humans in accordance with the local legislation and institutional requirements because only commercially available established cell lines were used. Since all the data used in the current study was available online, and no individual patient was involved, the IRB (Institutional Review Board) review was exempted.

Author contributions

XS: Data curation, Formal analysis, Funding acquisition, Investigation, Methodology, Project administration, Software, Writing – original draft. SX: Conceptualization, Data curation, Formal analysis, Project administration, Resources, Software, Supervision, Validation, Visualization, Writing – original draft. ZY: Conceptualization, Investigation, Methodology, Project administration, Resources, Visualization, Writing – review & editing. TZ: Formal analysis, Investigation, Methodology, Project administration, Resources, Writing – review & editing. TX: Data curation, Funding acquisition, Investigation, Methodology, Resources, Validation, Writing – review & editing.

Funding

Acknowledgments

Conflict of interest

The authors declare that the research was conducted in the absence of any commercial or financial relationships that could be construed as a potential conflict of interest.

Publisher's note

All claims expressed in this article are solely those of the authors and do not necessarily represent those of their affiliated organizations, or those of the publisher, the editors and the reviewers. Any product that may be evaluated in this article, or claim that may be made by its manufacturer, is not guaranteed or endorsed by the publisher.

References

1. Siegel RL, Miller KD, Wagle NS, Jemal A. Cancer statistics, 2023. *CA Cancer J Clin.* (2023) 73:17–48. doi: 10.3322/caac.21763

2. Adebayo AS, Agbaje K, Adesina SK, Olajubutu O. Colorectal cancer: disease process, current treatment options, and future perspectives. *Pharmaceutics.* (2023) 15:2620. doi: 10.3390/pharmaceutics15112620

3. Jung HS, Ryoo SB, Lim HK, Kim MJ, Moon SH, Park JW, et al. Tumor Size >5 cm and Harvested LNs <12 Are the Risk Factors for Recurrence in Stage I Colon and Rectal Cancer after Radical Resection. *Cancers (Basel).* (2021) 13:5294. doi: 10.3390/cancers13215294

4. Brouwer NP, Webbink L, Haddad TS, Rutgers N, van Vliet S, Wood CS, et al. Transcriptomics and proteomics reveal distinct biology for lymph node metastases and tumour deposits in colorectal cancer. *J Pathol.* (2023) 261:401–12. doi: 10.1002/path.6196

5. Crucitta S, Cucchiara F, Mathijssen R, Mateo J, Jager A, Joosse A, et al. Treatment-driven tumour heterogeneity and drug resistance: Lessons from solid tumours. *Cancer Treat Rev.* (2022) 104:102340. doi: 10.1016/j.ctrv.2022.102340

6. Qin Y, Rodin S, Simonson OE, Hollande F. Laminins and cancer stem cells: Partners in crime? *Semin Cancer Biol.* (2017) 45:3–12. doi: 0.1016/j.semcancer.2016.07.004

7. Mukwaya A, Jensen L, Lagali N. Relapse of pathological angiogenesis: functional role of the basement membrane and potential treatment strategies. *Exp Mol Med.* (2021) 53:189–201. doi: 10.1038/s12276-021-00566-2

8. Malta MD, Cerqueira MT, Marques AP. Extracellular matrix in skin diseases: The road to new therapies. *J Adv Res.* (2023) 51:149–60. doi: 10.1016/j.jare.2022.11.008

9. van Tienderen GS, Rosmark O, Lieshout R, Willemse J, de Weijer F, Elowsson Rendin L, et al. Extracellular matrix drives tumor organoids toward desmoplastic matrix deposition and mesenchymal transition. *Acta Biomater.* (2023) 158:115–31. doi: 10.1016/j.actbio.2022.11.038

10. Li S, Qi Y, McKee K, Liu J, Hsu J, Yurchenco PD. Integrin and dystroglycan compensate each other to mediate laminin-dependent basement membrane assembly and epiblast polarization. *Matrix Biol.* (2017) 57–58:272–84. doi: 10.1016/j.matbio.2016.07.005

11. Sherwood DR. Basement membrane remodeling guides cell migration and cell morphogenesis during development. *Curr Opin Cell Biol.* (2021) 72:19–27. doi: 10.1016/j.ceb.2021.04.003

12. Jayadev R, Morais MRPT, Ellingford JM, Srinivasan S, Naylor RW, Lawless C, et al. A basement membrane discovery pipeline uncovers network complexity, regulators, and human disease associations. *Sci Adv.* (2022) 8:eabn2265. doi: 10.1126/sciadv.abn2265

13. Tian W, Luo Y, Tang Y, Kong Y, Wu L, Zheng S, et al. Novel implication of the basement membrane for breast cancer outcome and immune infiltration. *Int J Biol Sci.* (2023) 19:1645–63. doi: 10.7150/ijbs.81939

14. Zhao Y, Yin Z, Huang K, Zhang F, Chen Y, Deng Y, et al. The basement membrane-related gene signature is associated with immunity and predicts survival accurately in hepatocellular carcinoma. *J Cancer Res Clin Oncol.* (2023) 149:5751–60. doi: 10.1007/s00432-022-04549-2

15. Wang J, Liu D, Wang Q, Xie Y. Identification of basement membrane-related signatures in gastric cancer. *Diagnostics (Basel).* (2023) 13:1844. doi: 10.3390/diagnostics13111844

16. Chen DT, Hernandez JM, Shibata D, McCarthy SM, Humphries LA, Clark W, et al. Complementary strand microRNAs mediate acquisition of metastatic potential in colonic adenocarcinoma. *J Gastrointest Surg.* (2012) 16:905–13. doi: 10.1007/s11605-011-1815-0

17. Lee HO, Hong Y, Etlioglu HE, Cho YB, Pomella V, Van den Bosch B, et al. Lineage-dependent gene expression programs influence the immune landscape of colorectal cancer. *Nat Genet.* (2020) 52:594–603. doi: 10.1038/s41588-020-0636-z

18. Liu Z, Liu L, Weng S, Guo C, Dang Q, Xu H, et al. Machine learning-based integration develops an immune-derived lncRNA signature for improving outcomes in colorectal cancer. *Nat Commun.* (2022) 13:816. doi: 10.1038/s41467-022-28421-6

19. Yoshihara K, Shahmoradgoli M, Martínez E, Vegesna R, Kim H, Torres-Garcia W, et al. Inferring tumour purity and stromal and immune cell admixture from expression data. *Nat Commun.* (2013) 4:2612. doi: 10.1038/ncomms3612

20. Liberzon A, Subramanian A, Pinchback R, Thorvaldsdóttir H, Tamayo P, Mesirov JP. Molecular signatures database (MSigDB) 3.0. *Bioinformatics.* (2011) 27:1739–40. doi: 10.1093/bioinformatics/btr260

21. Jiang P, Gu S, Pan D, Fu J, Sahu A, Hu X, et al. Signatures of T cell dysfunction and exclusion predict cancer immunotherapy response. *Nat Med.* (2018) 24:1550–8. doi: 10.1038/s41591-018-0136-1

22. Maeser D, Gruener RF, Huang RS. oncoPredict: an R package for predicting *in vivo* or cancer patient drug response and biomarkers from cell line screening data. *Brief Bioinform.* (2021) 22:bbab260. doi: 10.1093/bib/bbab260

23. Di Nicolantonio F, Vitiello PP, Marsoni S, Siena S, Tabernero J, Trusolino L, et al. Precision oncology in metastatic colorectal cancer - from biology to medicine. *Nat Rev Clin Oncol.* (2021) 18:506–25. doi: 10.1038/s41571-021-00495-z

24. Yang Y, Yang X, Ren S, Cao Y, Wang Z, Cheng Z. Identification and analysis of prognostic metabolic characteristics in colon adenocarcinoma. *Heliyon.* (2024) 10: e27388. doi: 10.1016/j.heliyon.2024.e27388

25. Zhang MH, Niu H, Li Z, Huo RT, Wang JM, Liu J. Activation of PI3K/AKT is involved in TINAG-mediated promotion of proliferation, invasion and migration of hepatocellular carcinoma. *Cancer biomark.* (2018) 23:33–43. doi: 10.3233/CBM-181277

26. Bernet A, Mazelin L, Coissieux MM, Gadot N, Ackerman SL, Scoazec JY, et al. Inactivation of the UNC5C Netrin-1 receptor is associated with tumor progression in colorectal Malignancies. *Gastroenterology.* (2007) 133:1840–8. doi: 10.1053/j.gastro.2007.08.009

27. Coissieux MM, Tomsic J, Castets M, Hampel H, Tuupanen S, Andrieu N, et al. Variants in the netrin-1 receptor UNC5C prevent apoptosis and increase risk of familial colorectal cancer. *Gastroenterology.* (2011) 141:2039–46. doi: 10.1053/j.gastro.2011.08.041

28. Gabasa M, Radisky ES, Ikemori R, Bertolini G, Arshakyan M, Hockla A, et al. MMP1 drives tumor progression in large cell carcinoma of the lung through fibroblast senescence. *Cancer Lett.* (2021) 507:1–12. doi: 10.1016/j.canlet.2021.01.028

29. Feng X, Wu Z, Wu Y, Hankey W, Prior TW, Li L, et al. Cdc25A regulates matrix metalloprotease 1 through Foxo1 and mediates metastasis of breast cancer cells. *Mol Cell Biol.* (2011) 31:3457–71. doi: 10.1128/MCB.05523-11

30. Chen Y, Peng S, Cen H, Lin Y, Huang C, Chen Y, et al. MicroRNA hsa-miR-623 directly suppresses MMP1 and attenuates IL-8-induced metastasis in pancreatic cancer. *Int J Oncol.* (2019) 55:142–56. doi: 10.3892/ijo

31. Held-Feindt J, Paredes EB, Blömer U, Seidenbecher C, Stark AM, Mehdorn HM, et al. Matrix-degrading proteases ADAMTS4 and ADAMTS5 (disintegrins and metalloproteinases with thrombospondin motifs 4 and 5) are expressed in human glioblastomas. *Int J Cancer.* (2006) 118:55–61. doi: 10.1002/ijc.21258

32. Rao N, Ke Z, Liu H, Ho CJ, Kumar S, Xiang W, et al. ADAMTS4 and its proteolytic fragments differentially affect melanoma growth and angiogenesis in mice. *Int J Cancer.* (2013) 133:294–306. doi: 10.1002/ijc.28037

33. Deichaite I, Sears TJ, Sutton L, Rebibo D, Morgan K, Nelson T, et al. Differential regulation of TNFα and IL-6 expression contributes to immune evasion in prostate cancer. *J Transl Med.* (2022) 20:527. doi: 10.1186/s12967-022-03731-x

34. Li X, Wang J, Zhang C, Lin C, Zhang J, Zhang W, et al. Circular RNA circITGA7 inhibits colorectal cancer growth and metastasis by modulating the Ras pathway and upregulating transcription of its host gene ITGA7. *J Pathol.* (2018) 246:166–79. doi: 10.1002/path.5125

35. Mehlen P, Bredesen DE. Dependence receptors: from basic research to drug development. *Sci Signal.* (2011) 4:mr2. doi: 10.1126/scisignal.2001521

36. Pun S, Ng YP, Yang JF, Ip NY, Tsim KW. Agrin-deficient myotube retains its acetylcholine receptor aggregation ability when challenged with agrin. *J Neurochem.* (1997) 69:2555–63. doi: 10.1046/j.1471-4159.1997.69062555.x

37. Zhang H, Liang J, Lu T, Li M, Shan G, Bi G, et al. AGRN promotes lung adenocarcinoma progression by activating Notch signaling pathway and acts as a therapeutic target. *Pharmacol Res.* (2023) 194:106819. doi: 10.1016/j.phrs.2023.106819

38. Ries C. Cytokine functions of TIMP-1. *Cell Mol Life Sci.* (2014) 71:659–72. doi: 10.1007/s00018-013-1457-3

39. Song G, Xu S, Zhang H, Wang Y, Xiao C, Jiang T, et al. TIMP1 is a prognostic marker for the progression and metastasis of colon cancer through FAK-PI3K/AKT and MAPK pathway. *J Exp Clin Cancer Res.* (2016) 35:148. doi: 10.1186/s13046-016-0427-7

40. Luo J, Lai C, Xu X, Shi J, Hu J, Guo K, et al. Mechanism of prognostic marker SPOCK3 affecting Malignant progression of prostate cancer and construction of prognostic model. *BMC Cancer.* (2023) 23:741. doi: 10.1186/s12885-023-11151-3